Electron spin resonance study on single crystals of orthoperiodic acid γ irradiated at room temperature

B Anusuya, V S Murty and K V S Rama Rao

Magnetism and Magnetic Materials Laboratory, Department of Physics, Indian Institute of Technology, Madras-600 036, India

Abstract. ESR studies have been performed on single crystals of orthoperiodic acid (H_5IO_6) in the X band at RT. New paramagnetic centres formed after γ-irradiation at RT are identified as IO_6^{4-} radicals trapped at two inequivalent sites, as could be seen from their g-values and hyperfine field values. The spin-density distributions of electrons on the s and p orbitals of iodine have been calculated.

1. Introduction

ESR spectroscopy has been widely used to probe the nature of paramagnetic centres trapped in salts containing non-metal oxy-anions [1]. Radicals formed after irradiation by γ-rays or x-rays in alkali-metal perchlorates and perbromates have been studied extensively [2–4]. However, very few iodates and periodates have been studied so far. The radical formed on γ-irradiation at RT in single crystals of potassium oxyfluoroiodate (KIO_2F_2) was first identified as IO_2F^- [5] and was later ascribed to IO_2 weakly interacting with a fluoride ion [6]. A species described as a neutral iodine atom (I^0) was trapped in x-irradiated single crystals of iodic acid (HIO_3) at RT [7]. The radical IO_3^{2-} was reported in single crystals of α-$LiIO_3$ γ irradiated at RT [8]. A paramagnetic species prepared from IO_4^- embedded in solid $KBrO_4$ by x-irradiation at 26 K was identified as IO_4^{2-} [9].

Orthoperiodic acid (H_5IO_6) is an interesting system wherein the IO_6, which has an octahedral arrangement, is slightly distorted, giving rise to a finite electric field gradient which is responsible for the observation of pure quadrupole resonance signals [10, 11]. An ESR study on powders of γ-irradiated periodates at 77 K has been reported and the electron loss centre in H_5IO_6 was identified as the $(HO)_5IO^- - OI(OH)_5^+$ radical and the electron gain centre was identified as the $H_5IO_6^-$ radical [12]. Here, we report the paramagnetic radical observed at RT by ESR in single crystals of H_5IO_6 γ irradiated at RT.

2. Crystal structure

Orthoperiodic acid belongs to the monoclinic crystal class with a space group $P2_1/n$. The lattice constants are $a = 5.28$ Å, $b = 18.35$ Å, $c = 4.95$ Å and $\beta = 111.4°$ [13, 14]. There are four molecules in the unit cell. The molecule of H_5IO_6 consists of a slightly deformed oxygen octahedron with iodine near the centre (figure 1(a)). Five of the oxygen atoms are directly linked to the hydrogen atoms. For these five oxygen atoms, the distance to the central iodine atom is 1.89 Å. For the remaining oxygen atom, the I–O(2) distance is

1.78 Å. It has been suggested that the bonds in the molecule may be covalent [14]. The O–H distances average to 0.96 Å. Each IO_6 octahedron is linked to the neighbouring IO_6 octahedra by ten hydrogen bonds (figure 1(b)). In the three-dimensional network which is thus formed, five independent hydrogen bonds may be distinguished.
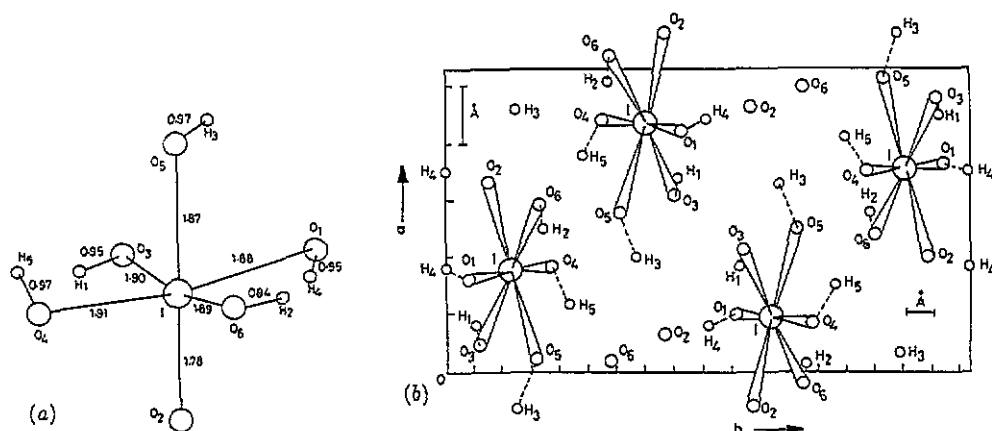

Figure 1. (a) The molecule of H_5IO_6, where the d-distances are given in ångströms. (b) Crystal structure of the H_5IO_6 projection in the c plane.

3. Experimental details

Single crystals of orthoperiodic acid were grown by evaporation of saturated aqueous solution. Since H_5IO_6 is highly hygroscopic, for irradiation at RT, the crystal was kept in a sealed tube and this was kept in the chamber of a ^{60}Co γ-ray source with a dose rate of 0.12 Mrad h^{-1}. The optimum irradiation dose for H_6IO_6 at RT was found to be 4 Mrad. The ESR spectra were recorded on a Varian E-112 X-band spectrometer operating with 100 kHz modulation. The ESR spectra were recorded by rotating the single crystal about the a, b and c^* (mutually perpendicular to the a and b axes) axes. The DPPH g-value of 2.0036 was used as an internal standard in evaluating the parameters g.

4. Results

No ESR spectra could be recorded at 300 K for the unirradiated crystals. Before γ-irradiation, the crystals were transparent but, after γ-irradiation, the crystals developed a slight yellow colouration. ESR spectra recorded at RT showed a six-line pattern spread over 1500 G. The spectra indicated a large (about 250 G) hyperfine interaction with a ^{127}I nucleus. The individual lines were about 15 G wide (figure 2). As the magnetic field explored the a–c^* and b–c^* planes, two distinguishable sites were observed. However, when the crystal was rotated in the a–b plane, only a single site could be observed (figure 3).
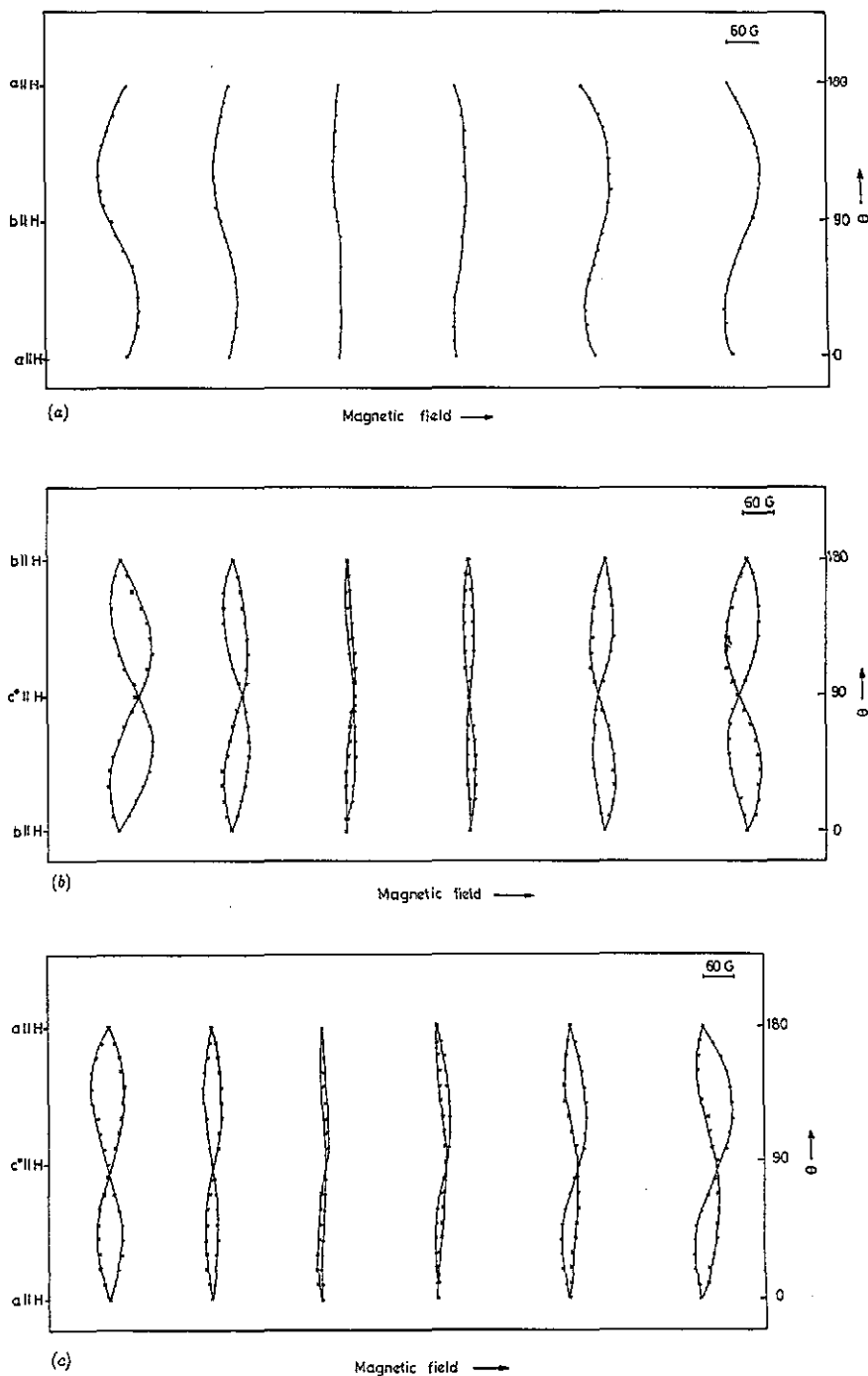
Figure 2. Variation in the resonance magnetic field with orientation for the six lines from the
^{127}I interaction in the spectrum of IO_6^{4-} for (a) the field in the a–b plane, (b) the field in the
b–c^* plane and (c) the field in the a–c^* plane.

5. Evaluation of ESR parameters

Since iodine has a reasonably large electric quadrupole moment as well as a large magnetic moment, we propose a Hamiltonian of the form

$$\mathcal{H}/g_0\beta_0 = (S_z g_z H_z + S_x g_x H_x + S_y g_y H_y)/g_0 + (S_z A_z I_z + S_y A_y I_y + S_x A_x I_x) + \mathcal{H}_Q/g_0\beta_0$$
(1)

where $\mathcal{H}_Q = e^2 q Q[3I_z - I(I+1) + \frac{1}{2}\eta(I_+^2 + I_-^2)]/[4I(2I-1)]$ and $eq = Q_{zz} = \delta^2 Q/\delta z^2$, $\eta = (Q_{xx} - Q_{yy})/Q_{zz}$. The term $S_z g_z H_z + S_x g_x H_x + S_y g_y H_y$ in equation (1) is the electron Zeeman term in which the g_i are the components of the g-tensor, and the term $S_z A_z I_z + S_y A_y I_y + S_x A_x I_x$ is the hyperfine interaction term in which the A_i are the components of the hyperfine tensor **A**, β_0 is the Bohr magneton, g_0 is the electron g-factor (2.0023), $\mathcal{H}_Q$ is the quadrupolar Hamiltonian and Q is the quadrupole moment [7].

The angular variation of the ESR spectra has been studied in three planes, namely the b–c^* plane, the a–b plane (which is perpendicular to the c^* axis) and the a–c^* plane. Measurements have been made on the positions of the line centres for every $10°$ in each of the above planes. The g-values were calculated from the mean position of the hyperfine lines. If l_1, l_2 and l_3 are the direction cosines of the magnetic field with respect to the a, b and c^* axes, then

$$g^2 = \sum_{i,j=1,2,3} R_{ij} l_i l_j = R_{11} l_1^2 + R_{22} l_2^2 + R_{33} l_3^2 + 2R_{12} l_1 l_2 + 2R_{23} l_2 l_3 + 2R_{13} l_1 l_3$$
(2)

where R_{ij} are the components of the g^2-tensor $[R]$ with respect to a, b and c^*.

In the b–c^* plane, let θ be the angle between the magnetic field and the c^* axis; $l_1 = 0$, $l_2 = \sin\theta$, $l_3 = \cos\theta$, and therefore

$$g^2 = R_{22} \sin^2\theta + R_{33} \cos^2\theta + 2R_{23} \sin\theta \cos\theta.$$

The values of g measured along the c^* axis and b axis give R_{33} and R_{22}. The value of R_{23} (and also the values of R_{22} and R_{33}) was found by multiple linear regression. Using the values of R_{22}, R_{33} and R_{23} in the above equation, the variation in g^2 with θ was calculated and the experimental g^2 variation is least squares fitted. The same procedure is repeated for the other two planes. Similarly, the hyperfine tensor matrix is also evaluated. Since g is not isotropic, the linear angular variation in $g^2 A^2$ is found instead of A^2. The principal values of the g-tensor and the ^{127}I hyperfine interaction tensor, together with their direction cosines relative to the crystallographic axes, were evaluated by the Jacobi pivotation method [18].

It can be seen from figure 3(a) that the experimental hyperfine spacings increase as the magnetic field goes from low to high. This could be due to the second-order field effect which arises when the magnitude of the hyperfine field is sufficiently large relative to the applied field or due to the quadrupole interaction effect. This effect has an m_I^2-dependence which produces a progressive increase or decrease in the hyperfine line spacings. Corrections for the second-order hyperfine effects were accounted for using the expression

$$H_0 = H_{m_I} + A m_I + A^2/2H_{m_I}[I(I+1) - m_I^2] + A^3/4H_{m_I}^2$$
(3)

where A is the true hyperfine splitting, H_{m_I} is the experimental line position for the transition $(M_s, m_I) \rightarrow (M_s^{\pm}, m_I)$ (since $\Delta M_s = \pm 1$ and $\Delta m_I = 0$), I is the nuclear spin and $g = h\nu/\beta H_0$.

These parameters were used in the second-order perturbation formulae given by Atherton and Winscom [15] to obtain the line positions. These compare well with the experimental line positions. The spectrum for a particular orientation in the a–b plane was simulated using the calculated field positions and the observed intensities (figure 4).
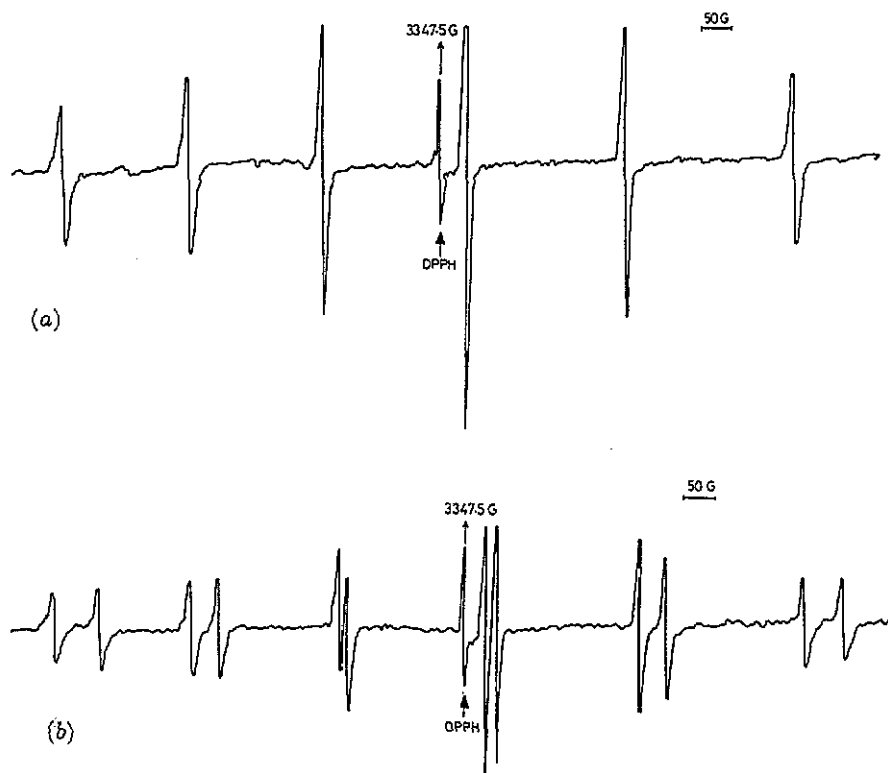
Figure 3. (a) First-derivative X-band spectrum of H_5IO_6 γ irradiated at RT and recorded at RT; the magnetic field is parallel to the c^* axis of the crystal. (b) First-derivative X-band spectrum of H_5IO_6 γ irradiated at RT and recorded at RT; the magnetic field is at an angle of 45° to the b axis.

6. Discussion and conclusion

The radical that we have observed in H_5IO_6, γ irradiated and recorded at RT is found to have g-values greater than 2.0023 (table 1). This indicates the formation of a hole centre. The radical does not show much variation in the hyperfine interaction values. The direction of one (g_{zz}) of the principal **g**-tensors almost coincides with one of the I–O bond directions, namely I–O(1) (table 2).

Since the ESR spectrum shows only six lines corresponding to the hyperfine interaction of the electron with one iodine nucleus, the possibility of an I_2^- centre can be eliminated [19]. The isotropic hyperfine interaction values reported for both electron loss and gain centres in powders of H_5IO_6 γ irradiated at 77 K [12] do not correspond to the hyperfine interaction value that we have observed for the radical at RT. The hyperfine interaction values reported for the radical ion IO_4^{2-} were very large [9]. The radical IO_3^{2-} reported in an α-$LiIO_3$ crystal gives a negative value for the anisotropic coupling [8]. The radical IO_2 observed in both $KClO_4$ [16] and KIO_2F_2 [5, 6] crystals shows a significant variation in the hyperfine interaction along the three principal directions. Thus, eliminating the probability of the above-mentioned iodine-containing radicals reported so far, we conclude that the radical in H_5IO_6 could have been formed as the result of the loss of one of the electrons as
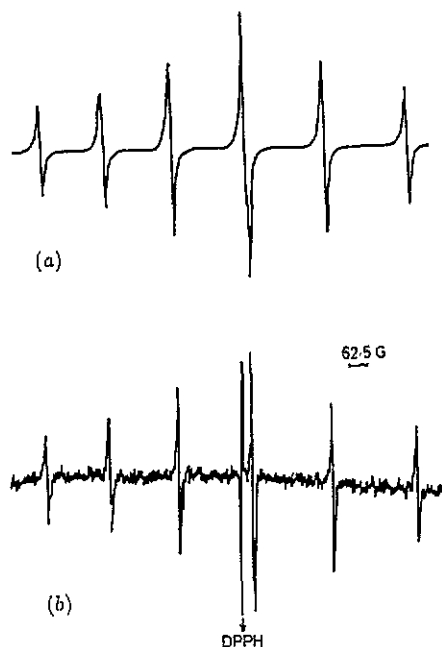
$$IO_6^{5-} + h\nu(\gamma) \rightarrow IO_6^{4-} + e^-. \tag{4}$$

Figure 4. (a) Computer-simulated spectrum for a random orientation in the a–b plane. (b) Experimental spectrum in the a–b plane.

Table 1. Spin-Hamiltonian parameters for the IO_6^{4-} radicals in γ-irradiated H_5IO_6 at RT.

	Principal g-values	Principal A-values (G)
IO_6^{4-}(A)	$g_{xx} = 2.0344$	$A_{xx} = 213.72$
	$g_{yy} = 2.0156$	$A_{yy} = 232.50$
	$g_{zz} = 2.0130$	$A_{zz} = 284.81$
IO_6^{4-}(B)	$g_{xx} = 2.0311$	$A_{xx} = 213.72$
	$g_{yy} = 2.0208$	$A_{yy} = 217.60$
	$g_{zz} = 2.0110$	$A_{zz} = 299.71$

	Principal axis	Direction cosines of the principal axes referred to the following a, b and c^* crystal axes		
		a	b	c^*
IO_6^{4-}(A)	x	0.7507	0.1543	0.6424
	y	0.5055	−0.7603	−0.4080
	z	0.4255	0.6310	−0.6487
IO_6^{4-}(B)	x	0.5014	0.5132	0.6966
	y	0.7785	−0.6189	−0.1044
	z	0.3776	0.5946	−0.7098

The experimental hyperfine splitting tensor for ^{127}I can be written in terms of isotropic and dipolar terms and the spin density in the iodine valence shell orbitals may be estimated from these components. The isotropic splitting arises from ground-state wavefunctions that

include small contributions from s orbitals. This can be estimated from

$$a = A_0\rho_{ns}^2 \tag{5}$$

where a is the measured value of the isotropic hyperfine interaction, A_0 is the calculated value of the isotropic hyperfine interaction for the case when the wavefunction is of pure s character and ρ_{ns}^2 is thus the probability of finding the electron in the s orbital [1]. The dipolar part of the hyperfine interaction arises owing to wavefunctions of non-spherical symmetry. We make an assumption that the unpaired electron on the iodine lies mostly in the 5p state and neglect the admixture of d-type wavefunctions.

Table 2. Direction cosines of the I–O bonds in H_5IO_6.

Bond	Direction cosines		
I–O(1)	0.3332	0.6909	−0.6415
I–O(2)	−0.9014	0.4165	0.1186
I–O(3)	0.3706	0.5830	0.7230
I–O(4)	−0.2761	−0.7307	0.6244
I–O(5)	0.8761	−0.4711	−0.1027
I–O(6)	−0.3058	−0.5898	−0.7474

Since the signs of the principal components of the tensor are not determined experimentally, we assume that the isotropic term will be positive, that the dipolar term will be approximately axial, of the form $(2B, -B, -B)$, and that the p-to-s ratio is within the range. The only choice of signs which is compatible with these assumptions is that all components are positive. Thus the hyperfine tensor could be split into a large positive isotropic interaction (+243.68 G) and a dipolar term with principal components $(-29.96, -11.18, +41.13)$. Any anisotropic hyperfine interaction can be written as resulting from the sum of any two perpendicular p wavefunctions. The p_x and p_z functions seem to be the best choices as the hyperfine interaction has approximately cylindrical symmetry around the x axis (table 1). Therefore, the experimental tensor will be interpreted as

$$\begin{vmatrix} 213.72 & & \\ & 232.50 & \\ & & 284.81 \end{vmatrix} = \begin{vmatrix} 243.68 & & \\ & 243.68 & \\ & & 243.68 \end{vmatrix} + \begin{vmatrix} -17.44 & & \\ & -17.44 & \\ & & 34.88 \end{vmatrix} + \begin{vmatrix} -12.52 & & \\ & 6.26 & \\ & & 6.26 \end{vmatrix}. \tag{6}$$

For ^{127}I, the isotropic and dipolar hyperfine interactions have been calculated by Hurd and Coodin [17] using the Hartree–Fock self-consistent method. Thus, for the iodine centre, the unpaired spin density in the iodine 5s and 5p orbitals can be estimated from $A_0 = 9277$ G and $2B_0 = 579.49$ G and it has been found that

$$\rho_{5s} = 0.0263 \qquad \rho_{5p_z} = 0.06 \qquad \rho_{5p_x} = 0.022.$$

This means that, between the s and p orbitals, only 10.79% of the electron wavefunction is accounted for. There is also a probability of finding the unpaired electron on the surrounding oxygen atoms.

Acknowledgments

References

[1]   Atkins P W and Symons M C R 1967 *The Structure of Inorganic Radicals* (Amsterdam: Elsevier)
[2]   Byberg J R and Jensen S J K 1975 *J. Chem. Phys.* **52** 5902–10
[3]   Byberg J R 1971 *J. Chem. Phys.* **55** 4867–72
[4]   Bloom M B D, Eachus R S and Symons M C R 1970 *J. Chem. Soc.* A 1235–8
[5]   Subramanian S and Rogers M T 1971 *J. Phys. Chem.* **75** 3479–85
[6]   Atherton N M, Morton J R, Preston K F and Strach S J 1981 *J. Chem. Phys.* **74** 5521–5
[7]   Bailey C E 1973 *J. Chem. Phys.* **59** 1599–606
[8]   Martirosyan V O, Meilman M L, Marov I N and Shukov V V 1975 *Phys. Status Solidi* b **68** 791–5
[9]   Byberg J R 1987 *J. Chem. Phys.* **86** 6065–9
[10] Rama Rao K V S and Weiss Al 1971 *Z. Naturf.* a **26** 1813–6
[11] Ramaprabhu S, Rama Rao K V S and Weiss Al 1983 *J. Mol. Struct.* **111** 295–300
[12] Symons M C R and Mishra S P 1981 *J. Chem. Soc., Dalton Trans.* 2183–7
[13] Feikema Y D 1961 *Acta Crystallogr.* **14** 315–6
[14] Feikema Y D 1966 *Acta Crystallogr.* **20** 765–9
[15] Atherton N M and Winscom C J 1973 *Inorg. Chem.* **12** 383–90
[16] Byberg J R 1986 *J. Chem. Phys.* **85** 4790–3
[17] Hurd C M and Coodin P 1967 *J. Phys. Chem. Solids* **28** 523–5
[18] Misra S K 1984 *Physica* B **124** 53–61
[19] Boesman E and Shoemaker D 1962 *J. Chem. Phys.* **37** 671–2